

Session XI
Thursday, September 8 - morning
I11
X-RAY NANO-FOCUSING FOR COHERENT IMAGING: MEET YOUR PROBE
Tim Salditt
Institut für Röntgenphysik, Universität Göttingen

Advanced X-ray optics and focusing opens us the potential of hard X-rays structure analysis, which is unique in terms of penetration, spatial resolution, contrast, and compatibility with environmental conditions was significantly. With the advent of highly brilliant radiation, coherent X-ray focusing, and lens-less diffractive imaging, we can now probe local structures selectively, even in hierarchical environment such as biological cells and tissues.

We illustrate central challenges and advances of hard X-ray nano focusing for coherent imaging, and present a compound optical system consisting of elliptical mirrors and X-ray waveguides. The setup enables full field projection imaging at high magnification down to 20 nm resolution [1], but can also cover a three-dimensional field of view, large enough to probe thick tissues with sensitivity to single cells and sub-cellular structures [2]. The required inversion of the coherent diffraction pattern can be mastered

by different reconstruction algorithms in the optical far and near-field.

In this talk we focus on advanced waveguide x-ray optics [3] for coherent imaging, and on the characterisation of the illumination system (probe) by different ptychographic reconstruction schemes, both in the far- and near-field.

1. M. Bartels, M. Krenkel, J. Habe, R.N. Wilke, T. Salditt: X-Ray Holographic Imaging of Hydrated Biological Cells in Solution, *Phys. Rev. Lett.* **114**, 048103 (2015).
2. M. Krenkel, A. Markus, M. Bartels, C. Dullin, F. Alves, T. Salditt: Phase-contrast zoom tomography reveals precise locations of macrophages in mouse lungs, *Sci.Rep.* **5**, 09973 (2015).
3. T. Salditt, S. Hoffmann, M. Vassholz, J. Haber, M. Osterhoff, J. Hilhorst: X-Ray Optics on a Chip: Guiding X Rays in Curved Channels, *Phys. Rev. Lett.* (2015), 115, 203902.

C34
X-RAY WAVEGUIDE ARRAYS: TAILORED NEAR-FIELDS BY MULTI-BEAM INTERFERENCE
Q. Zhong¹, T. Salditt¹, M. W. Wen², Z. S. Wang²

¹*Institut für Röntgenphysik, Universität Göttingen, Friedrich-Hund-Platz 1, 37077 Göttingen, Germany*
²*MOE Key Laboratory of Advanced Micro-Structured Materials, Institute of Precision Optical Engineering, Department of Physics, Tongji University, Shanghai 200092, China*
 tsalditt@gwdg.de

X-ray waveguides enable a variety of X-ray optical functions, from beam collimation to below 10 nm [1] and coherence filtering [2], as required for high resolution holographic X-ray imaging [3], to beam splitting [4] for interferometry, beam tapering [5] or angular redirections [6]. While the guided X-ray beams are well controlled in the waveguide device, the exit near-field distribution is governed by free-space propagation and diffraction broadening, and hence is always much wider than in the waveguide

itself, which limits many interesting applications in imaging, diffraction or spectroscopy with nanometer sized X-ray beams.

In this work we show that by exploiting multi-waveguide interference, the near-field distribution behind the waveguide exit can be tailored for special properties, for example in view of creating a secondary focal spot. To this end we use an array of 7 planar waveguides, with precisely varied guiding layer thickness variation, as fabricated by

Table 1. The designed layer thickness values of the x-ray waveguide array (WGA).

Name	Ge sub	Mo	C	Mo												
Layer/nm		50.0	4.0	56.0	6.2	53.8	7.6	52.4	8.0	52.4	7.6	53.8	6.2	56.0	4.0	50.0

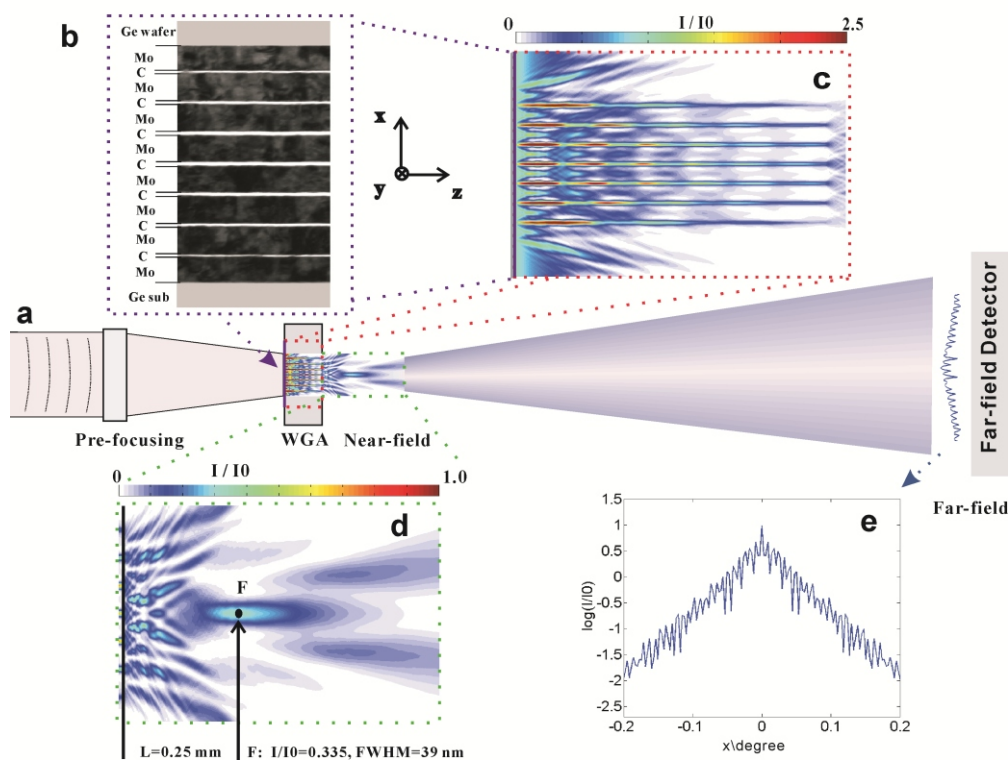


Figure 1. Setup and numerical simulations. (a) Schematic of experimental setup. The X-ray waveguide array (WGA) is positioned in at the focal plane of beamline optics. The incoming beam with 19.9 keV photo energy and primary intensity I_0 , is coupled into the X-ray waveguide array, which tailors the near-field to the desired shape. The far-field intensity distribution is recorded at a distance of 0.97m behind the WGA exit by a one-dimensional pixel detector (Mythen, Dectris). (b) The structure of the WGA as visualized by its TEM cross section of WGA. The WGA shown has seven C layers (guiding layers) and eight Mo layers (cladding layers), as detailed in Table 1. The optical layers are sandwiched by Ge wafers; (c) Using finite-difference simulations, the simulated wave propagation in the WGA is shown (intensity values). A plane wave is coupled into the front side of WGA, with a length of 300 μm from entrance to exit. (d) Simulations of the beam near the exit of the WGA, showing the multi-beam interference as tailored by the different phases. The focus point (F) is located at 0.25 mm behind the exit of WGA, with a normalized intensity $I/I_0 = 0.335$ and a width (full width of half maximum, FWHM) of 39 nm). (e) The simulated far field pattern.

high precision magnetron sputtering of amorphous carbon and molybdenum. The controlled thickness variations in the range of 0.1 nanometers resulting in a desired phase shift of the different waveguide beams. In this way, special effects such as a single or a double focus or tilted emission of the beam can be achieved by multi-beam interference. In contrast to the previously used resonant beam coupling (RBC) for waveguides with multiple guiding layers [7], the present design based on front coupling of a pre-focused beam is much more versatile. Fig.1 visualizes the general concept of the X-ray waveguide arrays (WGA) with corresponding numerical simulations. The detailed layers thickness values of an example WGA structure are shown in Tab. 1. This structure was simulated and measured using bending magnet radiation at the European Synchrotron Radiation Facility (ESRF) in Grenoble (data not shown).

Our study which includes numerical simulations, design, fabrication, and experimental results demonstrates that X-ray waveguide arrays can be used to tailor an X-ray near-field distribution. In particular, multi-beam interference with phase shifts controlled by variation of guiding layer thickness can lead to beam intensity maximum in free space behind the waveguide exit with a spot size (FWHM) in the sub-50nm range. The simulated near-field is compared to the reconstructed field based on the measured far-field (in progress).

1. S. P. Krueger, H. Neubauer, M. Bartels, S. Kalbfleisch, K. Giewekemeyer, P. J. Wilbrandt, M. Sprung, T. Salditt, *Journal of Synchrotron Radiation*, **19**, (2012), pp. 227-236.
2. M. Osterhoff, T. Salditt, *New Journal of Physics*, **13**, (2011), 103026.
3. M. Bartels, M. Krenkel, J. Haber, R.N. Wilke, T. Salditt, *Physical Review Letters*, **114**, (2015), 048103.
4. C. Fuhse, C. Ollinger, T. Salditt, *Physical Review Letters*, **97**, (2006), 254801.
5. H.-Y. Chen, S. Hoffmann, T. Salditt, *Applied Physics Letters*, **106**, (2015), 194105.
6. T. Salditt, S. Hoffmann, M. Vassholz, J. Haber, M. Osterhoff, J. Hilhorst, *Physical Review Letters*, **115**, (2015), 203902.
7. F. Pfeiffer, T. Salditt, P. Hřghřj, I. Anderson, N. Schell, *Physical Review B*, **62**, (2000), pp. 16939-16943.

We thank Mike Kanbach for help in waveguide processing, Markus Osterhoff and Sarah Hoffmann for help during the beamtime at the ROBL beamline of ESRF, and Hsin-Yi Chen and Lars Melchior for help the finite-difference simulations. We gratefully acknowledge the German Research Foundation (DFG) for funding through Grant No. SFB 755, the German Ministry of Research BMBF through Verbundforschung Großgeräte Synchrotronstrahlung, and the China Scholarship Council of P.R. China for financial support.

SINGLE NANOWIRE X-RAY DIFFRACTION ANALYSIS IN ENSEMBLE MEASUREMENTS

J. Vogel¹, A. Davtyan¹, L. Feigl², J. Jakob², S. M. Mostafavi Kashani^{1,2}, P. Schroth^{1,2}, T. Baumbach^{2,3,4} and U. Pietsch¹

¹Department of Physics, University of Siegen, Emmy-Noether Campus, Walter-Flex-Str. 3, 57072 Siegen, Germany

²Institute for Photon Science and Synchrotron Radiation, KIT - Karlsruhe Institute of Technology, Hermann-von-Helmholtz-Platz 1, 76344 Eggenstein-Leopoldshafen, Germany

³Laboratory for Applications of Synchrotron Radiation, KIT - Karlsruhe Institute of Technology, Kaiserstr. 12, 76131 Karlsruhe, Germany

⁴Synchrotron Radiation Facility ANKA, KIT - Karlsruhe Institute of Technology, Hermann-von-Helmholtz-Platz 1, 76344 Eggenstein-Leopoldshafen, Germany
jonas.vogel@student.uni-siegen.de

In a current project we are aiming to study the growth of a single semiconductor nanowire (NW) by in-situ X-ray diffraction. Here we report on recent experiments performed at beamline P09 of PETRA III using a portable MBE chamber. By time resolved reciprocal space mapping in the vicinity of the symmetric GaAs (111) and asymmetric (220) and (311) zinc-blende and (10.3) wurtzite Bragg reflections, the evolution of self-catalysed GaAs NWs on silicon substrates has been monitored. Single NWs were studied using pre-patterned substrates with a lateral spacing of five microns prepared by focused ion beam hole drilling.

Two different approaches were tested to investigate single NWs:

1) A set of Compound Refractive Lenses (CRL) with focal length of 0.75m mounted on a hexapod was used resulting in a beam size of at the centre of the growth chamber. With this approach we were able to select single NWs (see Fig. 1, 1)).

2) Another set of CRL equipped 13.5m upstream the sample focused the beam without major divergence to a size of. Although this setup illuminated simultaneous an ensemble of NWs, single objects could be separated because of the rather parallel beam and the small vertical misalignments of individual NWs with respect to the growth direction (see Fig.1, 2)).

In this work we report on X-ray diffraction data taken from single GaAs NWs using both methods. In particular,

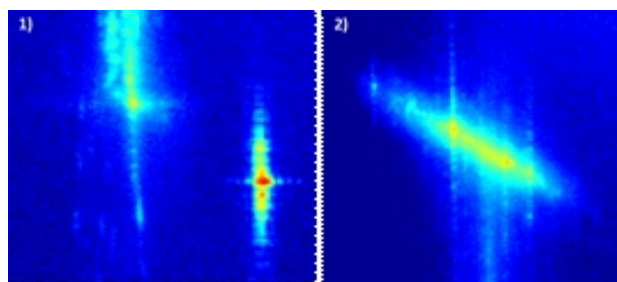


Figure 1. Comparison of X-ray diffraction in the vicinity of the GaAs (10.3) wurtzite reflection. Single objects are visible for both methods 1) (microfocus) and 2) (ensemble).

we recorded reciprocal space maps at symmetric and asymmetric Bragg peaks with settings 1) and 2) and compare the data in terms of resolution in reciprocal space and integrated intensity. In addition we compare both settings with respect to the capability of determining phase composition of a single NW [1]. Figure 1 shows separated X-ray diffraction signals in the vicinity of the (10.3) wurtzite reflection with focused beam using method 1) and ensemble measurements 2).

1. P. Schroth, M. Köhl, J.-W. Hornung, E. Dimakis, C. Somaschini, L. Geelhaar, A. Biermanns, S. Bauer, S. Lazarev, T. Baumbach and U. Pietsch, *Physical Review Letters*, **114**, (2015), 055504.



C36

DEFECT-ASSISTED X-RAY MICROSCOPY WITH POLYCAPILLARY OPTICS

P. Korecki, K. M. Sowa, B. R. Jany, F. Krok

Institute of Physics, Jagiellonian University, Lojasiewicza 11, 30-348 Krakow, Poland

Polycapillary X-ray focusing devices are built from hundreds of thousands of bent glass micro-capillaries that are stacked into hexagonal arrays. Defects were identified as to deteriorate the X-ray transmission of these devices. In this presentation, we demonstrate that natural point defects in the optics (missing, crushed, squeezed or larger capillaries) directly lead to the formation of multiple X-ray images of an object, which was positioned in the focal plane of the optics (see Fig 1). These multiple images can be analysed using the so called coded aperture approach [1-3]. The resulting spatial resolution is limited by the defect size and not by the focal spot size, which has typically size of 10-100 μm . In a recent proof-of-principle experiment [4] of defect-assisted microscopy, using a commercially available optics, we obtained sub-micron resolution that has not been achieved with focusing polycapillary optics until now. Tailored optics with a controlled distribution of “defects” (fabricated using procedures known from photonic crystal fibers [5]) could be used for multimodal nanoscale X-ray imaging with laboratory setups.

1. K. M. Dabrowski, D. T. Dul, and P. Korecki, *Opt. Express* **21**, (2013), 2920.
2. K. M. Dabrowski, D. T. Dul, A. Wrobel, and P. Korecki, *Appl. Phys. Lett.* **102**, (2013) 224104.
3. P. Korecki, T. P. Roszczynialski, and K. M. Sowa, *Opt. Express* **23**, (2015), 8749.
4. P. Korecki, K.M. Sowa, B. R. Jany, F. Krok, *Phys. Rev. Lett.* (2016), accepted for publication.
5. P. Russell, *Science* **299**, (2003) 358.

This work was supported by the Polish National Science Center (grant No. DEC-2013/11/B/ST2/04057).

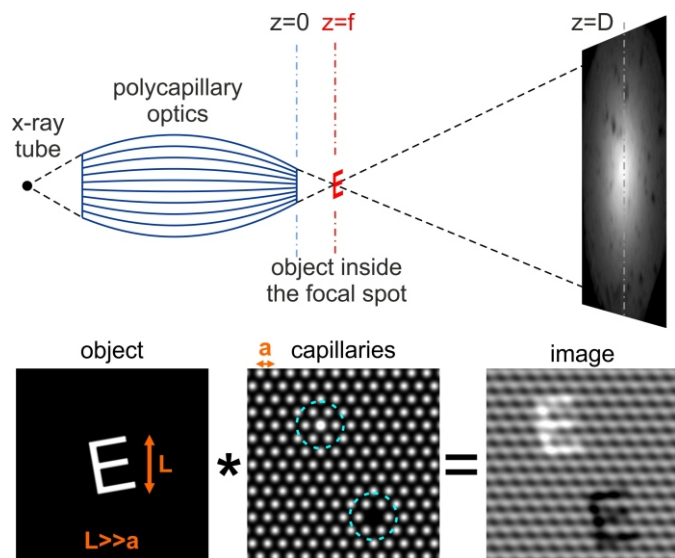
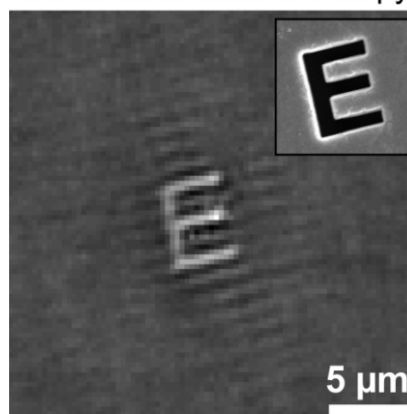


Figure 1. Idea of defect-assisted X-ray microscopy. Defects (missing or broken and larger capillaries - marked with dashed circles) break the periodicity and lead to the formation of distinct multiple x-ray images of the object.

defect-assisted microscopy



standard x-ray projection

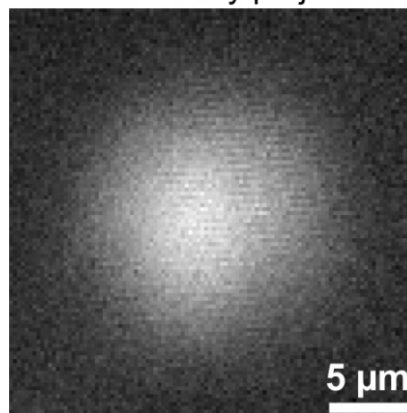


Figure 2. Comparison of defect-assisted imaging with standard X-ray projection imaging with the focal spot acting as a secondary source. Inset: SEM image of the object.

C37

SINGLE-SHOT-MULTIPROJECTION SETUP FOR ULTRAFAST AND ULTRAINTENSE IMAGING

P. Villanueva-Perez¹, B. Pedrini¹, R. Mokso², P. R. Willmott^{1,3}, V. Guzenko¹, C. David¹, and M. Stampanoni^{1,4}

¹Paul Scherrer Institut, Villigen, Switzerland

²MedMAX, Max IV Laboratory, Lund University, Sweden

³Experimenta Physics Institute, UZH Zurich, Zurich, Switzerland

⁴Institute for Biomedical Engineering, UZH/ETH Zurich, Zurich, Switzerland

The ultrashort and ultraintense pulses provided by X-ray free electron lasers enable to overcome the resolution limitations due to radiation damage for imaging biological materials [1]. Since each pulse destroys the sample, the accessible information in standard imaging approaches is limited to a single projection. We propose an experimental setup for the hard X-ray regime which permits the simultaneous acquisition of multiple projections from the same specimen, similar to that for soft X-rays in Ref. [2], exploiting the simultaneous illumination of the sample with multiple beams generated from the direct beam by a single crystal (see Figure). This technique thus allows acquisition of 3-D information from single-shot measurements.

We provide an experimental proof-of-principle of this concept at a synchrotron source in both coherent diffraction imaging and holographic geometries. For the former, implementation at X-ray free-electron laser is straightforward.

1. R. Neutze et al., *Nature* **406**, 752-757 (2000).
2. M. R. Howells and C.J. Jacobsen, Workshop on scientific applications of coherent X-rays SLAC-R-437, 159-162 (1994).

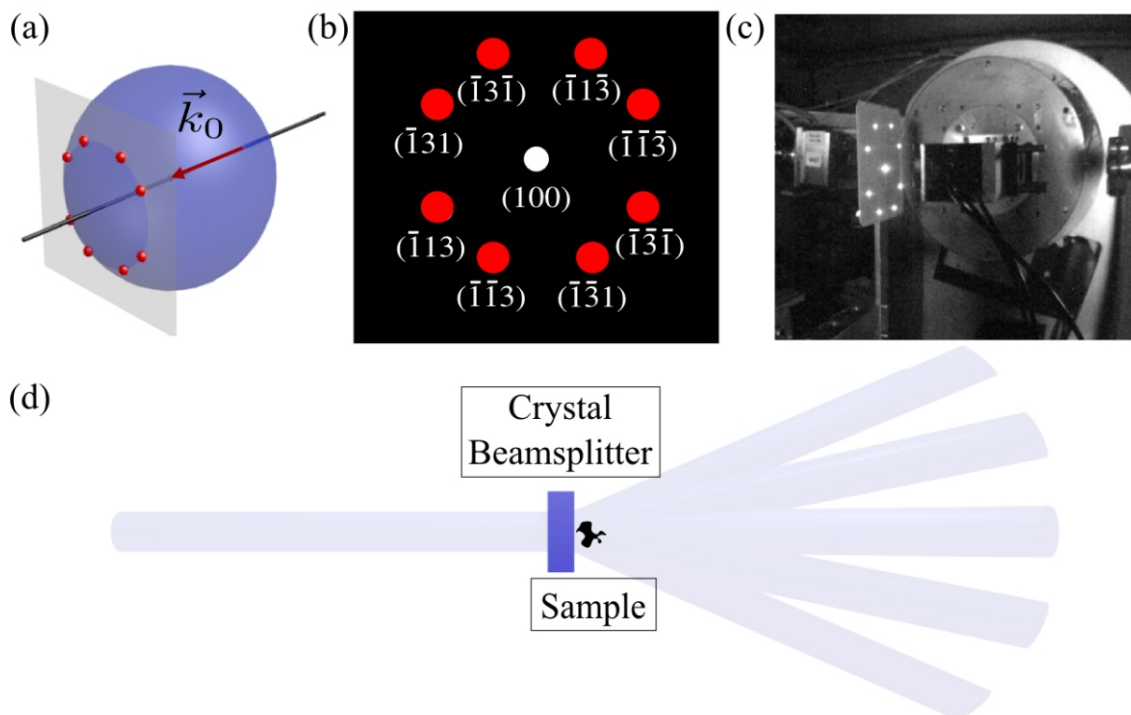


Figure 1: (a) Ewald sphere intersecting simultaneously a family of equivalent Bragg reflections, related by rotations around a symmetry axis of the silicon crystal. (b) Family of reflections in Bragg condition for a cubic lattice. (c) Picture of the experimental setup at the MS beamline of the Swiss Light Source, showing the hummer and the eight diffracted beams on a phosphor screen. (d) Sketch of the concept of the sample being illuminated simultaneously by the direct and diffracted beams.